O.K. KOPIYKA, V.V. KALINCHAK, A.S. CHERNENKO

Odesa I.I. Mechnikov National University
*(2, Dvoryans'ka Str., Odesa 65026, Ukraine; e-mail: teplophys@onu.edu.ua)*

# EVAPORATION OF DROPLETS OF BINARY MIXTURES OF LOWER MONOHYDRIC ALCOHOLS IN HEATED AIR

*The results obtained while studying the evaporation process of single droplets of lower alcohols – ethanol, butanol, and their binary mixtures – with initial droplet sizes of 1.5–2.5 mm in heated air at the atmospheric pressure are reported. It is shown that the second inflection points in the time dependences of the temperature and the squared droplet diameter allow the evaporation time interval to be divided into two stages: 1) the simultaneous evaporation of both alcohols with a higher content of the more volatile alcohol and 2) the evaporation of the less volatile alcohol. The application of a thermocouple, which was heated in the oven under experimental conditions, diminished the droplet evaporation time and increased the stationary temperature of the droplet evaporation. At air temperatures higher than the boiling point of the liquid fuel, the temperature difference between the gaseous medium and the evaporating droplet surface depended linearly on the gaseous environment temperature. We propose a formula for calculating the evaporation temperature for a droplet of a binary solution in heated air, which allows estimating the temperature at which the quasi-stationary evaporation of the droplet begins provided a low rate of temperature growth. In the calculations, temperature dependence of the specific vaporization heats and the difference of the Lewis number from unit. The emphasis is made on the necessity of taking the Stefan flow into account when performing the physical and mathematical simulations.*

*K e y w o r d s*: evaporation, alcohols, solution, droplet, thermocouple.

## 1. Introduction

The evaporation rate for a droplet of a binary solution consisting of two different liquid components is not constant and changes in time, because each component evaporates at a different rate. This phenomenon is called "selective evaporation" [1]: the more volatile component evaporates faster, because it has a higher saturated vapor pressure near the droplet surface. During such an evaporation of a droplet, the composition of the latter changes.

In recent decades, when determining the concentrations of components during the droplet evaporation, changes in the geometry of a droplet lying on a certain surface were studied [1–3]. One of the characteristic parameters is the contact angle, the angle between the droplet–air boundary and the surface, which is governed by the surface tensions at the interfaces between the contacting phases. However, in such studies, an important factor is the state of the surface, where the droplet is placed. For example, as was shown in work [4], the evaporation of droplets

from dry and lubricated surfaces is qualitatively different, which manifests itself in different rates at which the geometric parameters of the droplet (its wetting ridge and height) change.

Aqueous solutions of alcohols (ethanol, methanol, butanol) [5–8] and binary solutions of various alcohols (isopropanol and butanol) [9] are often used as research objects in such studies. In the case of binary mixtures of water and ethanol [3], three evaporation stages with different wetting characteristics were identified. The more volatile component evaporates completely at the first stage, whereas the less volatile component mainly does it at the last stage.

The challenging character of such studies is associated with the requirements of various technological processes and the real-life applications, where a surface is wetted with droplets and afterward dried out. For example, these are the inject printing [10], spraying of pesticides with the alcohol admixture on leaves [11], and medical diagnostics [12].

The overwhelming majority of the studies dealing with the evaporation of droplets of various liquids and their mixtures are carried on at room temperature [13–17]. This allows the contribution of various factors (convection, mixture composition, impurities, substrate or suspension, laser radiation, and so forth) to this process to be analyzed very carefully, because, as a rule, the evaporation rates at low temperatures are not high, and there is no need to complicate the laboratory thermostating equipment.

The evaporation of droplets at elevated temperatures is interesting, first of all, owing to its direct relation to the ignition and combustion processes [18–20]. When studying the burning processes of the droplets of a one-component liquid fuel, the droplet temperature is usually assumed to be practically equal to the fuel boiling point.

The study of the evaporation of mono- and multi-component fuel droplets remains a challenging task. The main existing theoretical models of the droplet evaporation are most completely expounded in Sazhin's review [17]. They are based on the analytic solution of the diffusion equation outside and inside the liquid droplet. When describing the heat exchange and the evaporation of droplets – for example, dodecane droplets of diameters down to 10 $\mu$m in a heated environment at a pressure of 30 atm [17, p. 133] – it was shown that they continued to evaporate until the temperature reached a stationary value. No calcula-

tion results were presented for larger, e.g., millimeter-size droplets. When determining the mass fraction of the fluid vapor, the dependence of the molar mass of the gas mixture on its temperature and composition was not taken into account as well.

When studying the evaporation of water droplets 1–3 mm in diameter in air with a temperature of 500–1000 K [21], it was shown that the temperatures at the surface of the droplet and inside it are substantially lower than the boiling temperature. The influence of the thermocouple (with a junction 10 times smaller than the characteristic size of the droplet) on the droplet evaporation time (a reduction by 3.5%) was noted. The studies of the evaporation of water droplets on the thermocouple also showed that the temperature field in the droplet is mainly formed during the initial heating time interval, when the temperatures at the center of the droplet and at its surface reach certain constant values.

In work [22], on the example of the evaporation of a droplet of a binary solution of $n$-heptane and $n$-decane, a change in the slope of the time dependence of the squared droplet diameter was shown, which was associated with the evaporation of $n$-heptane from the droplet. The authors of work [23] calculated the influence of the thermocouple diameter ($\leq 100$ $\mu$m) on the time dependence of the temperature of an $n$-dodecane droplet evaporating in heated air. The heating rate of the droplet and the stationary temperature of its evaporation decrease, as thermocouple diameter increases, because the heat outflow through the thermocouple due to its thermal conductivity increases with the growth of the thermocouple diameter. When comparing with the results of numerical calculations, the evaporation model developed by Abramzon and Sirignano [17] was used. It was shown that, at the beginning of the evaporation, the temperatures at the surface and at the center of a droplet differ by 90 K. When the droplet is heated to the stationary evaporation temperature, the temperature gradient disappears owing to the circulation inside the droplet. This is just at this time that the $d^2$-law (Sreznevsky's law) becomes relevant.

In work [24], the results were reported concerning a comparison between the experimental data obtained for the evaporation rates of water droplets and the values calculated in the framework of the classical kinetic diffusion and evaporation models, as well as an ordinary approach based on the empirical expres-
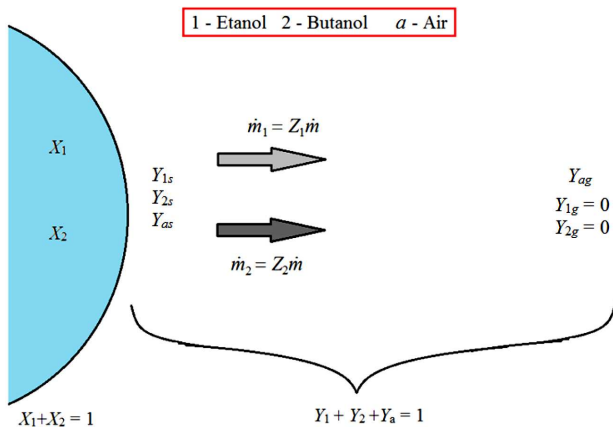
**Fig. 1.** Schematic diagram of the "solution droplet–air" system. $X_i$ $(i = 1, 2)$ is the mass fraction of the $i$-th component in the droplet, $Y_{is}$ $(i = 1, 2, a)$ is the mass fraction of the $i$-th component in air, $Y_{ig}$ $(i = 1, 2, a)$ is the mass fraction of the $i$-th component, and $Z_i$ $(i = 1, 2)$ is the fraction of the $i$-th component in the total evaporation mass flow

sions $\mathrm{Nu} = f(\mathrm{Pr}, \mathrm{Re})$. At moderate temperature values (lower than 600 K), the theoretical evaporation rates are in satisfactory agreement with the experimental ones (the difference does not exceed 15%). However, at temperatures above 1000 K, those evaporation rate values are several times different.

The authors of work [25] numerically simulated the heating of single droplets (10–100 $\mu$m in diameter) of a three-component kerosene substitute in a stationary heated (500–2000 K) environment at pressures of 0.3–10 atm. The obtained time dependences of the temperature and the squared droplet diameter made it possible to analyze the self-ignition and evaporation times of the droplet. Net evaporation was found to mainly depend on the gas temperature.

The authors of work [26] compared two models of the droplet evaporation developed on the basis of the Maxwell–Fuchs model. The old model considers the heat exchange of the droplet with the environment making use of the classical Newton–Richmann law. In the new model, the heat exchange coefficient accounts for the non-stationary character of heat exchange and the influence of evaporation on this process. Numerical results were reported for several primary reference hydrocarbons ($n$-heptane, $n$-decane, $n$-dodecane, and $n$-tetradecane) at gas temperatures from 400 to 1500 K and pressures from 1 to 40 MPa. According to the cited authors, the new model provides the more realistic characteristic times

of droplet heating and evaporation. Nevertheless, the obtained results contain a number of shortcomings. In particular, the droplet temperature was evaluated using an approximate transcendental equation, which is valid, if the temperatures of the droplet surface and, therefore, the surrounding gas are low. As a result, in the calculations, the surface temperature of the droplet during its evaporation in heated air began to exceed the boiling point. Moreover, the spontaneous ignition is possible for the examined hydrocarbons in heated air, which remained beyond the authors' attention.

Alcohols are widely used in internal combustion engines as additives to diesel fuel or gasoline [27, 28]. Most often, these are lower alcohols such as methanol or ethanol. Nevertheless, other alcohols such as propanol, $n$-butanol, and 1-pentanol are components of the next biofuel generation. They are considered to provide better fuel properties than lower alcohols do.

The aim of this study is to determine the specific features of the evaporation of the droplets of binary solutions of monoatomic alcohols at elevated temperatures. This process is considered as a preliminary stage before the fuel ignition in heated chambers. As research objects, droplets of ethanol, butanol, and their mixtures in stationary heated air are dealt with. The droplets were placed on a thermocouple surface, and the thermocouple was arranged in an oven.

## 2. Mass Exchange of a Droplet

Consider a spherical droplet of a binary solution. The droplet radius equals $r_s$, which is larger than the free path length of molecules in the gas phase surrounding the droplet (Fig. 1). We assume that the evaporation of each solution component from the droplet surface occurs independently with the formation of a saturated layer. This layer, besides the binary mixture components ethanol (the subscript 1) and butanol (the subscript 2), also includes air (the subscript $a$). Then, $Y_{1s} + Y_{2s} + Y_{as} = 1$, where $Y_i = \rho_i/\rho_g$ is the mass fraction of the component in the gas phase, $\rho_i$ is the partial density of the $i$-th component, and $\rho_g$ is the average mixture density. Hereafter, the subscript $s$ means the value of the relevant quantity near the droplet surface.

The velocity $u$ of the Stefan flow at the distance $r$ from the droplet center can be expressed in terms of

the droplet evaporation rate $\dot{m}$:

$$4\pi r^2 \rho_g u = \dot{m}_1 + \dot{m}_2 = \dot{m}.$$

Taking the Stefan flow [17, 29] into account, the mass and heat flows in the gas phase through any spherical surface of the radius $r > r_s$ can be written in the form

$$\dot{m}_i = -4\pi r^2 D_{gi}\rho_g \frac{dY_i}{dr} + 4\pi r^2 u\rho_g Y_i, \tag{1}$$

$$\dot{Q} = -4\pi r^2 \lambda_g \frac{dT}{dr} + 4\pi r^2 u\rho_g c_{pg}T =$$

$$= \sum_i \dot{m}_i L_i + 4\pi r_s^2 u_s \rho_{gs} c_{pg} T_s. \tag{2}$$

Hereafter, the subscript $i$ marks the quantities related to the $i$-th component of the fuel mixture; $\dot{m}_i = -dm_i/dt$ is the mass flow of the component, i.e., its evaporation rate; $D_{gi}$ is the diffusion coefficient of the vapor in the environment.

The mass flow $\dot{m}_i$ of the $i$-th component from the droplet surface is coupled with the total evaporation rate of the droplet $\dot{m}$ via the formula $\dot{m}_i = Z_i\dot{m}$, where $Z_i$ is the share of the mass flow of the $i$-th component in the total mass flow. Then, after integrating Eq. (1) with the boundary conditions $Y_i = Y_{is}$ at $r = r_s$, and $Y_{ig} = 0$ at $r \to \infty$, we obtain that the mass evaporation rate of a droplet with the diameter $d = 2r_s$ equals

$$\dot{m} = 2\pi d \frac{\text{Sh}}{2} D_{gi}\rho_g \ln(1 + B_i), \tag{3}$$

where
$$B_i = \frac{Y_{is}}{Z_i - Y_{is}},$$

is the Spalding number for the mass transfer, and Sh is the Sherwood number. Hence, for the $i$th component of the mixture,

$$\dot{m}_i = 2\pi d \frac{\text{Sh}}{2} D_{gi}\rho_g Z_i \ln(1 + B_i). \tag{4}$$

As a result, the droplet size and mass decrease according to the equations

$$-\frac{d(d)}{dt} = \frac{4}{d}\frac{\text{Sh}}{2}\frac{D_{gi}\rho_g}{\rho_L}\ln(1 + B_i),$$
$$\dot{m} = -\frac{d\left(\pi\rho_L d^3/6\right)}{dt}, \quad d(t=0) = d_0. \tag{5}$$

where $\rho_L$ is the droplet density.

The values of the mass evaporation rate and the rate of droplet diameter change should not depend on the choice of the $i$-th component in formulas (3) and (5). The assumption of the equality of the diffusion coefficients of the components in the gas phase $(D_{g1} \approx D_{g2})$ means the equality of the component Spalding numbers, $B_1 \approx B_2$. This latter equality brings us to the conclusion that the mass flows of the components from the droplet are interrelated as the mass concentrations of their saturated vapors:

$$\frac{\dot{m}_1}{\dot{m}_2} = \frac{Z_1}{Z_2} = \frac{Y_{1s}}{Y_{2s}}.$$

Taking into account that $Z_1 + Z_2 = 1$, we have

$$Z_i = \frac{Y_{is}}{Y_{1s} + Y_{2s}}. \tag{6}$$

According to Dalton's law $p'_1 + p'_2 + p'_a = P_0$, the equation of state for the ideal gas $\rho_i = \frac{\mu_i p'_i}{RT}$, and Raoult's law $p'_{is} = X_{\nu i}p_{is}$, the mass fraction of each alcohol in the mixture near the droplet surface is proportional to the molar fraction $X_{\nu i}$ of the component in the solution, the partial pressure $p_{is}$ of the saturated vapor of the pure component, and the ratio between the molar masses of the components, $\mu_i$, in the gas mixture at the droplet surface, $\bar{\mu}_{gs}$:

$$Y_{is} = \frac{\rho_i}{\bar{\rho}_g} = X_{\nu i}\frac{\mu_i p_{is}}{\bar{\mu}_{gs}P_0} =$$
$$= X_{\nu i}\frac{\mu_i p_{is}}{\mu_1 X_{\nu 1}p_{1s} + \mu_2 X_{\nu 2}p_{2s} + \mu_a\left(P_0 - p'_1 - p'_2\right)}. \tag{7}$$

Here, $P_0 = 10^5$ Pa is the atmospheric pressure, $p'_i$ is the partial pressure of the $i$-th component above the solution surface, and $X_i$ is the mass fraction of the $i$-th component of the binary solution in the droplet:

$$X_i = \frac{m_i}{m_1 + m_2}, \quad X_1 + X_2 = 1, \quad X_{\nu i} = \frac{\frac{X_i}{\mu_i}}{\frac{X_1}{\mu_1} + \frac{X_2}{\mu_2}}.$$

The common solution of the system of equations composed of two Eqs. (7) written for two solution components makes it possible to obtain the following corrected expression for the concentration of the saturated vapor near the droplet surface:

$$Y_{is} = X_{\nu i}\frac{\mu_i p_{is}}{\mu_a\left(1 + k_a\right)P_0}, \tag{8}$$

where
$$k_a = X_{\nu 1}\frac{\mu_1 p_{1s}}{\mu_a P_0}\left(1 - \frac{\mu_a}{\mu_1}\right) + X_{\nu 2}\frac{\mu_2 p_{2s}}{\mu_a P_0}\left(1 - \frac{\mu_a}{\mu_2}\right).$$

The correction $k_a$ increases (decreases) proportionally to the difference between the molar masses of each component and air. In particular, for the case of individual liquid vaporization ($X_{\nu 1} = 0$ or $X_{\nu 2} = 0$) at low air temperatures ($p_{1s} \ll P_0$), we have $k_a \approx 0$, and the molar mass of the mixture is equal to the molar mass of air, which can be seen from the comparison of Eqs. (7) and (8). At high temperatures ($p_{1s} \approx P_0$), we have $1 + k_a \approx \mu_1/\mu_a$, and the molar mass of the mixture is close to the molar mass of the vapor.

When the droplet is surrounded by a heated gaseous environment, it is necessary to consider the temperature dependence of the vaporization heat. To within an error of 2%, this dependence can be determined using Watson's formula [30]. In the temperature interval from 0 °C to the liquid boiling point, this formula can be linearly approximated as follows [29]:

$$L_T = L_{T_0} \left( \frac{T_{\rm cr} - T}{T_{\rm cr} - T_0} \right)^{0.38} \approx L_{T_0} - A(T - T_0), \qquad (9)$$

where

$$A = \frac{0.38 L_{T_0}}{T_{\rm cr} - T_0},$$

$T_{\rm cr}$ is the critical liquid temperature (in K units), and $T_0$ is some characteristic temperature. For ethanol, $L_{273K} = 951$ kJ/kg and $T_{\rm cr} = 514$ K; and for butanol-1, $L_{273K} = 736$ kJ/kg and $T_{\rm cr} = 563$ K. The necessity to take this temperature dependence into account is evidenced by the 13%-difference between the vaporization heats at 273 K and the boiling point for ethanol, the corresponding 30%-difference for butanol.

Substituting expression (9) into the Clausius–Clapeyron law in the differential form,

$$\frac{dp}{dT} = \frac{(L_{T_0} - A(T - T_0))\, \mu}{RT^2} p, \qquad (10)$$

and solving this equation, we obtain the temperature dependence of the saturated vapor pressure $p_{is}$ over the surface of a pure liquid in the form [29]

$$p_{is} = P_0 \exp \left[ \frac{L_{T_0 i} \mu_i}{R} \left( \frac{1}{T_{bi}} - \frac{1}{T_s} \right) \right] \left( \frac{T_s}{T_{bi}} \right)^{-\frac{A_i \mu_i}{R}} \times$$

$$\times \exp \left[ \frac{A_i \mu_i T_0}{R} \left( \frac{1}{T_{bi}} - \frac{1}{T_s} \right) \right]. \qquad (11)$$

where $T_{bi}$ is the boiling point of the $i$-th component, and $T_s$ is the droplet surface temperature. Thus, in formula (11), unlike to the usual exponential temperature dependence

$$p_{is} = P_0 \exp \left[ \frac{L \mu_i}{R} \left( \frac{1}{T_{bi}} - \frac{1}{T_s} \right) \right], \qquad (12)$$

which is obtained provided that the vaporization heat is constant, we have a correction factor that takes the temperature dependence of the specific vaporization heat into account. If we assume that the function $L_T(T)$ changes weakly with the temperature ($L_T(T) \approx$ const), this will substantially simplify the integration of Eq. (10) and will allow its direct substitution into formula (12). As a result, both expression (12), taking the dependence $L_T(T)$ into account and expression (11) are in accurate agreement (with an error not exceeding 10%) with the following empirical dependences [31]:
for ethanol,

$$\lg p_s = 7.81 - \frac{1919}{T - 21};$$

and for butanol-1,

$$\lg p_s = 8.72 - \frac{2265}{T + 7};$$

where $p_s$ is reckoned kPa units.

## 3. Heat Exchange of a Droplet

A droplet of the binary solution was suspended on a thermocouple. The droplet temperature (assuming that it does not differ from the average droplet temperature) changes and reaches a stationary value according to the differential equation

$$\frac{4}{3} \pi r_s^3 \rho_L c_L \frac{dT_s}{dt} = \lambda_g 4\pi r^2 \left. \frac{\partial T_g}{\partial r} \right|_{r=r_s} -$$

$$- L_1 \dot{m}_1 - L_2 \dot{m}_2 + N Q_m \qquad (13)$$

with

$$T_s(0) = T_b.$$

The first term on the right-hand side of Eq. (13) describes the heat flow coming to the droplet surface from the environment, the second and third ones the heat that is spent for the droplet evaporation, and the

fourth one the heat that arrives through the thermo-couple electrodes ($N = 2$). In order to determine the temperature gradient in the gas near the droplet surface, it is necessary to solve the equation of thermal conductivity in the gas phase accounting for the Stefan flow and the boundary conditions at the droplet surface and at the boundary of the reduced film:

$$\frac{d}{dr}\left(4\pi r^2 \lambda_g \frac{dT_g}{dr}\right) = \frac{d}{dr}\left(4\pi r^2 U \rho_g c_{pg} T_g\right), \qquad (14)$$

with

$$T_g\left(r = r_s\right) = T_s, \quad T_g\left(r = r_f\right) = T_{g\infty},$$

where $\lambda_g$ is the coefficient of thermal conductivity in the gas [W/(m K)], $T_g$ is the gas temperature [K], and $r_f$ is the radius of the reduced film.

In the framework of the quasi-stationary thermal model, while determining the mass evaporation rate for the droplet in the first approximation, the following condition is assumed to be obeyed at the droplet surface: all heat coming from the environment to the droplet is spent for the evaporation,

$$L_1 \dot{m}_1 + L_2 \dot{m}_2 = \lambda_g 4\pi r^2 \left.\frac{dT_g}{dr}\right|_{r=r_s}. \qquad (15)$$

Doubly integrating Eq. (14) from $r_s$ to $r$ and taking condition (15) into account bring us about the following expression for the mass evaporation rate of the droplet:

$$\dot{m} = \frac{4\pi r_s \lambda_g}{c_{pg}\left(1 - r_s/r_f\right)} \ln\left[1 + \frac{c_{pg}\left(T_{g\infty} - T_{gs}\right)}{L_1 Z_1 + L_2 Z_2}\right]. \qquad (16)$$

Therefore, the heat flow from the environment to the droplet equals

$$\lambda_g 4\pi r^2 \left.\frac{dT_g}{dr}\right|_{r=r_s} = 4\pi r_s^2 \frac{\lambda_g \mathrm{Nu}}{2r_s} \frac{L_1 Z_1 + L_2 Z_2}{c_{pg}} \times$$
$$\times \ln\left(1 + \frac{c_{pg}\left(T_{g\infty} - T_s\right)}{L_1 Z_1 + L_2 Z_2}\right),$$

where $\mathrm{Nu} = 2/\left(1 - r_s/r_f\right)$ is the Nusselt criterion. Just this expression is used, when describing the heat exchange of an evaporating droplet consisting of a pure liquid [17]. Then Eq. (13) for the temperature change of a spherical droplet of a binary solution during its evaporation into a gaseous environment takes the form

$$\rho_L c_L \pi \frac{d^3}{6} \frac{dT_s}{dt} = \pi d^2 \frac{\lambda_g \mathrm{Nu}}{d} \frac{L_1 Z_1 + L_2 Z_2}{c_{pg}} \times$$

$$\times \ln\left(1 + \frac{c_{pg}\left(T_{g\infty} - T_s\right)}{L_1 Z_1 + L_2 Z_2}\right) - \sum_i L_i \dot{m}_i + N Q_m. \qquad (17)$$

with

$$T_s\left(t = 0\right) = T_{s0}.$$

To estimate the heat transfer through the thermocouple electrodes, the following differential equation describing the thermal conductivity through a long thin cylinder with the simultaneous convective heat transfer can be considered:

$$\lambda_m \frac{d^2 T}{dx^2} = \frac{2\alpha}{r_B}\left(T - T_{g\infty}\right), \quad \alpha = \frac{\lambda_g \mathrm{Nu}_m}{2r_m},$$

with

$$T(x = 0) = T_s, \quad T(x = \infty) = T_{g\infty},$$

where $r_m$ is the thermocouple radius, $x$ is the distance from the given cross-section to the droplet, $\lambda_m$ is the thermal conductivity of the thermocouple material, and $\mathrm{Nu}_m$ is the Nusselt criterion (we put $\mathrm{Nu}_m = 0.5$). The amount of heat coming to the droplet through the thermoelectrode per unit time is determined from the expression

$$Q_m = \pi r_B^2 \lambda_m \left.\frac{dT}{dx}\right|_{x=0} = \pi r_B \lambda_B \sqrt{\frac{2\alpha r_B}{\lambda_B}}\left(T_{g\infty} - T_s\right).$$

A chromel-alumel thermocouple of the K-type and 200 $\mu$m in diameter was used. At 20 °C, the thermal conductivity of both alloys equals $\lambda_m = 17.6$ W/(m·K).

Inside the film, the following temperature dependences were used for the required parameters:

• for the diffusion coefficients of the components,

$$D_{gi} = D_{gi0}\left(\frac{T_s + T_{g\infty}}{2T_0}\right)^{n_i};$$

• for the density,

$$\rho_g = \rho_{g0}\frac{2T_0}{T_s + T_{g\infty}};$$

• and for the thermal conductivity coefficient of the gas mixture,

$$\lambda_g = \lambda_{g0}\left(\frac{T_s + T_{g\infty}}{2T_0}\right)^{n_0};$$

where $T_{g\infty}$ is the ambient temperature.

The density and the specific heat of a droplet are determined as follows:

$$\rho_L = \left(\frac{X_1}{\rho_1} + \frac{X_2}{\rho_2}\right)^{-1}$$

and

$$c_L = X_1 c_1 + X_2 c_2,$$

respectively. Similarly to the specific vaporization heats, the temperature dependences $\rho_L(T)$ and $c_L(T)$ for ethanol and butanol in an interval of 273–473 K can be approximated by the expressions [32]

$$\rho_1 \left[\text{kg/m}^3\right] = 804 - 0.659\,(T - 273) - $$
$$- 2.66 \times 10^{-3}(T - 273)^2,$$

$$\rho_2 \left[\text{kg/m}^3\right] = 825 - 0.709\,(T - 273) - $$
$$- 1.42 \times 10^{-3}(T - 273)^2,$$

$$c_1 \left[\text{J/(kg} \times \text{K)}\right] = 2270 - 5.44\,(T - 273) + $$
$$+ 4.89 \times 10^{-2}(T - 273)^2,$$

$$c_2 \left[\text{J/(kg} \times \text{K)}\right] = 2200 + 7.09\,(T - 273) + $$
$$+ 3.16 \times 10^{-2}(T - 273)^2.$$

The system of equations (5) and (17) was solved numerically using the finite difference method. Other calculation parameters are $D_{g10} = 10 \times 10^{-6}$ m$^2$/s, $D_{g20} = 7.1 \times 10^{-6}$ m$^2$/s, $\rho_{g0} = 1.29$ kg/m$^3$, $\lambda_{g0} = 0.0224$ W/(m $\times$ K), $T_{b1} = 351$ K, $T_{b2} = 391$ K, $n_i = 1.75$, and $n_0 = 0.75$.

In the limiting cases, when the concentration of either of the mixture components is taken equal to zero, the model makes it possible to describe the evaporation of a one-component fuel.

## 4. Analysis of Numerical Results

The results obtained while solving the system of equations (5) and (17) for the evaporation of droplets of the binary (50/50 wt%) mixture of ethanol and butanol with an initial diameter of 1.4 mm are depicted in Fig. 2. The evaporation temperature of the droplet of the binary solution does not remain constant. It is in the dependences of the droplet diameter on the temperature rather than on the time, where the differences in the evaporation of the droplets of a one-component liquid fuel and a binary solution manifest themselves.

The analysis was carried out with and without accounting for the influence of thermoelectrodes. The final sections of curves *1* in Fig. 2 were plotted as dashed curves, because the minimum size of the droplet during its evaporation cannot be smaller than the size of the thermocouple junction. It is evident that the additional heat supply via the thermocouple affects the rate of the process. However, the main features do not change.

In particular, each of the time dependences of the droplet temperature and squared diameter (Figs. 2, *a–d*) has two inflection points at the same time coordinates. The extremes in the time dependences of $\frac{d}{dt}d^2$ are weakly pronounced: the evaporation constant remains practically constant even for the binary solution. In order to determine why they appear, it is necessary to consider the time behavior of the droplet and gas mixture compositions (Figs. 2, *e–f*).

Provided the equal initial contents of ethanol and butanol in the droplet (Fig. 2, *e*), the vapor near the droplet surface at the initial evaporation stage mainly consists of ethanol (Fig. 2, *f*). As the droplet temperature increases in time, the amount of ethanol in the near-surface layer increases. As a result of the competition between two opposite processes (the growth of the droplet temperature and the reduction of the ethanol content in the droplet), the ethanol surface concentration $Y_{1s}$ reaches a maximum value. This is the origin of the appearance of the first inflection point in the dependence $T(t)$.

The second inflection point is associated with an increase of the butanol concentration in the near-surface layer and its equalization with the ethanol concentration. Above this point, the vapor in the near-surface layer mainly consists of butanol vapor.

## 5. Experimental Study of Evaporation of Droplets on a Thermocouple

The droplet was suspended on a chromel-alumel thermocouple with a thermoelectrode thickness of 200 $\mu$m. With the help of a special mechanism, it was introduced through a hole into the upper part of a horizontally located hermetic oven, where a constant temperature of heated air was maintained. The oven was illuminated through its transparent side wall with white light. A contrast image of the droplet was reg-
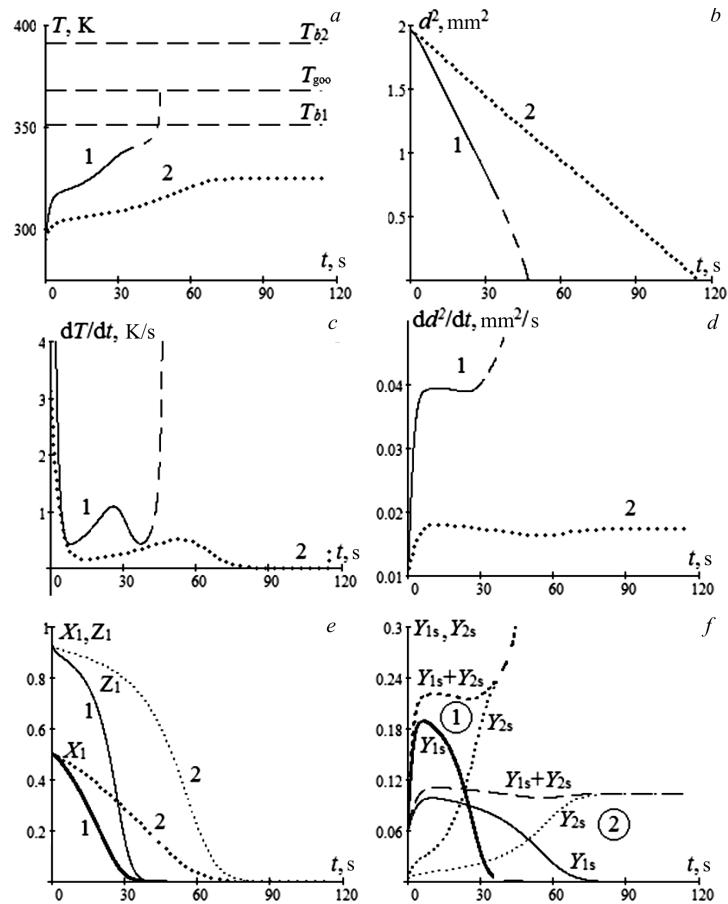
**Fig. 2.** Evaporation kinetics of the droplets of the binary solution of ethanol and butanol (50/50 wt%) in air at the temperature $T_{g\infty} = 368$ K: the droplet temperature ($a$), the droplet squared diameter ($b$), the time derivative of the droplet temperature ($c$), the time derivative of the droplet squared diameter ($d$), the mass fraction $X_1$ of ethanol in the solution and the mass fraction $Z_1$ of ethanol in the total mass flow during the evaporation ($e$), the surface concentrations of the saturated ethanol (subscript 1) and butanol (subscript 2) vapors ($f$). Curves *1* correspond to a droplet on a thermocouple, and curves *2* to a free droplet. The initial temperature of the droplets is 295 K, and the diameter is 1.4 mm

istered through the other side of the oven making use of a web camera. As a result, the droplet appeared dark against a light background. The digital image processing made it possible to obtain the time dependence of the droplet diameter. The thermocouple readings were registered using a Picotest300 multivoltmeter at a frequency of 5 values per second.

The experiments were performed at three different air temperatures: 368, 485, and 565 K (Fig. 3). The autoignition temperatures in air are 677 K for ethanol and 613 K for butanol. In both cases, the droplet temperature did not exceed the boiling point of the less volatile component (the boiling points are 351 K for ethanol and 391 K for butanol). As the droplet size

approached the thermocouple junction size, the thermocouple readings approached the temperature of the heated medium. Furthermore, butanol remnants on the junction evaporated very slowly at lower air temperatures. Therefore, the droplet diameters after the end of the evaporation were substantially different (see Fig. 2, *b*).

From Fig. 2, one can see that, in the framework of this model, the stationary temperature of the droplet on the thermocouple is higher than the corresponding value in the absence of a thermocouple. This result contradicts the results of work [23]. However, in work [23], the droplet was first suspended on the cold junction of a thermocouple and afterward introduced into
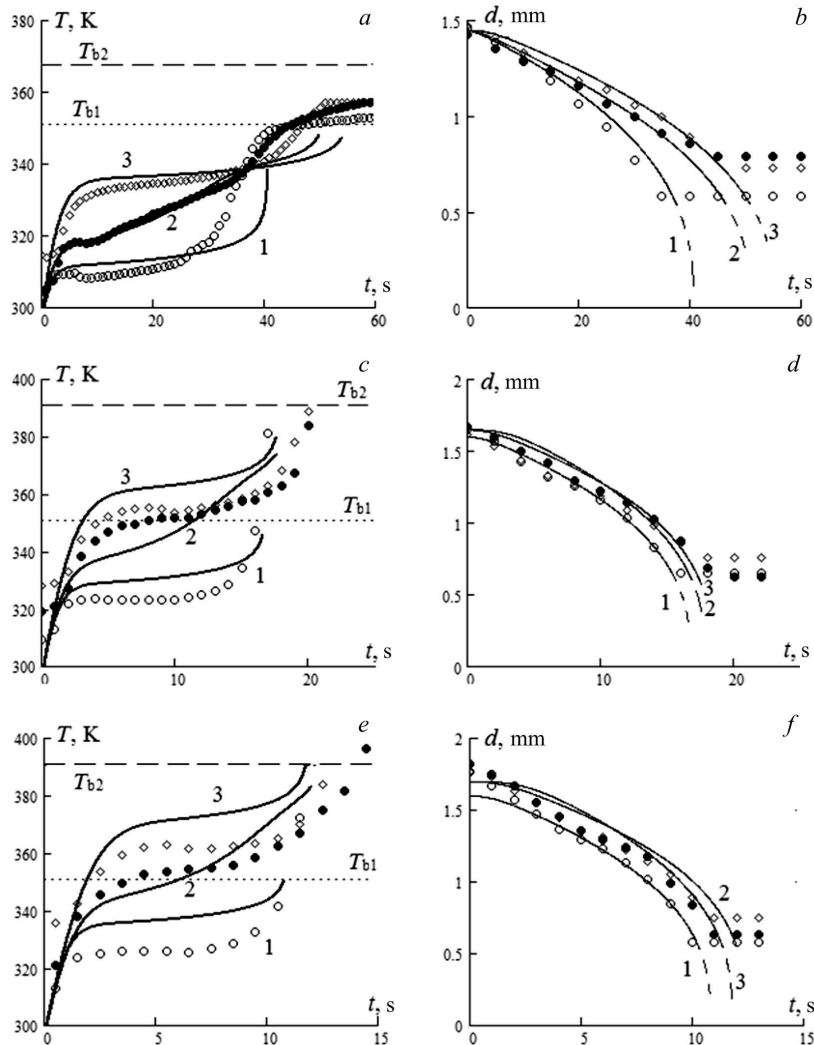
**Fig. 3.** Time dependences of the temperature $(a, c, e)$ and diameter $(b, d, f)$ of the droplets of ethanol (hollow circles), binary solution 50% ethanol + 50% butanol (solid circles), and butanol (diamonds) in air at temperatures of 368 $(a, b)$, 485 $(c, d)$, and 565 K $(e, f)$. Solid curves demonstrate the results of numerical calculations taking into account heat losses through the thermocouple; symbols correspond to experimental data

the oven. Therefore, the thermocouple electrodes did not have enough time to heat up significantly, so the heat was taken out through the thermocouple.

In our studies, droplets with a definite composition were also suspended on a thermocouple and introduced into a heated oven. However, immediately after the first droplet had evaporated, the thermocouple was removed from the oven, and the next droplet was hung on the junction. This procedure was repeated several times. As a result, the dependences registered for the first droplet were always substan-

tially different from the subsequent ones, which were identical. This occurred, because, during the first experimental cycle, the thermocouple electrodes were gradually heated up near the droplet almost to the temperature of the medium. In further cycles, the thermoelectrodes were already heated, and heat was supplied to the droplet through them. The model described by Eqs. (5) and (17) makes allowance for the presence of heated thermocouple electrodes.

The presence of a moderately volatile alcohol in the solution leads to the situation where, as the temper-
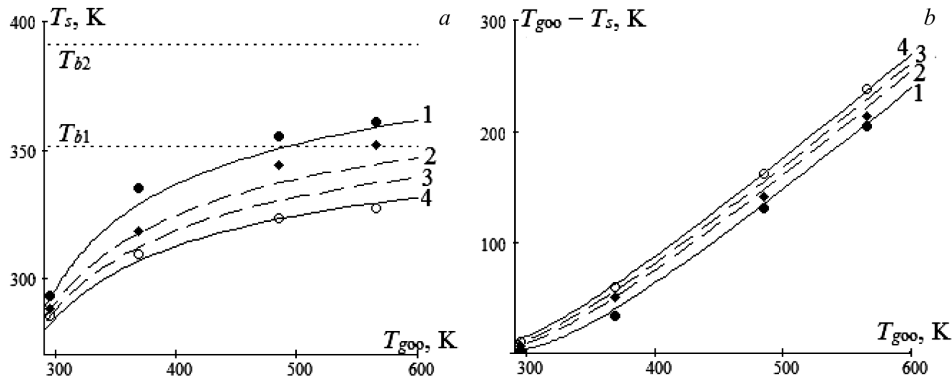
**Fig. 4.** Dependences of the stationary droplet evaporation temperature on the air temperature. Calculation by Eq. (17): (*1*) 100% butanol, (*2*) 75% butanol + 25% ethanol, (*3*) 50% butanol + + 50% ethanol, and (*4*) 100% ethanol. Experimental data: (solid circles) 100% butanol, (diamonds) 50% butanol + 50% ethanol, and (hollow circles) 100% ethanol

ature of the gas medium increases, the temperature of the droplet during its evaporation approaches the boiling point of the highly volatile alcohol and can exceed it, only if the content of the latter in the solution substantially decreases.

The temperature of a droplet of a binary solution of ethanol and butanol changed monotonically from the evaporation temperature of pure ethanol to the evaporation temperature of pure butanol. However, it was possible to distinguish separately the stage of droplet heating and the next stage, when the rate of temperature change was much lower. This change is associated with a change in the droplet composition. The evaporation temperature of a droplet of a binary solution was closer to the evaporation temperature of the less volatile component.

At the same time, the changes of the droplet diameter were practically the same within the experimental error.

## 6. Analytic Evaluation of the Temperature of One-Component Fuel Droplet

In order to determine the stationary temperature $T_s$ of the droplet surface during the evaporation, it is enough to put zero the right-hand side of Eq. (17) without taking the heat transfer through the thermocouple electrodes into account. As a result, we obtain the equation

$$\ln\left(1 + \frac{c_{pg}\,(T_{g\infty} - T_s)}{L_1 Z_1 + L_2 Z_2}\right) =$$

$$= \frac{\text{Sh}}{\text{Nu}}\text{Le}\,\ln\left(\frac{1}{1 - (Y_{1s} + Y_{2s})}\right), \tag{18}$$

where

$$Z_i = \frac{Y_{is}}{Y_{1s} + Y_{2s}}, \quad i = 1, 2,$$

and Le is the Lewis number. This expression also demonstrates the equality of the rates of liquid mass evaporation in the framework of the thermal and diffusion models.

The exact analytic solution of Eq. (18) is complicated due to the exponential (Arrhenius-type) temperature dependence of the quantities $Y_s$. However, this equation can be rewritten as the dependence of the medium temperature on the droplet one:

$$T_{g\infty} = T_s + \frac{L_1 Z_1 + L_2 Z_2}{c_{pg}} \times$$

$$\times \left(\left(\frac{1}{1 - Y_{1s} - Y_{2s}}\right)^{\text{Le}\frac{\text{Sh}}{\text{Nu}}} - 1\right). \tag{19}$$

The relevant Lewis numbers are Le = 0.578 for ethanol and Le = 0.418 for butanol. The ratio between the Nusselt and Sherwood numbers depends on the convection level. For instance, $\text{Nu}/\text{Sh} \approx 1$ in the case of film flow, and $\text{Nu}/\text{Sh} \approx \text{Le}^m$, where $m = 0.33$, if the blowing velocities are low.

In Fig. 4, *a*, the calculated and experimental dependences $T_s(T_{g\infty})$ are depicted. As the temperature of the gas medium increases, the droplet evaporation temperature monotonically approaches the boiling temperature, but does not exceed it. It is the use

**Stationary temperatures of droplets, $T_s$ [K], at their evaporation in heated air**

| Alcohol | $T_s$, K | Numerical calculation of the system of equations (5) and (17) | | Calculation of $T_s$ by | | | Experiment on a chromel-alumel thermocouple | |
|---|---|---|---|---|---|---|---|---|
| | | without suspension | with suspension | (18) | (19) | (20) | $T_s$, K | $T_g - T_s$, K |
| Ethanol | 295 | 278 | 285 | 282 | 282 | 282 | 285 | 10 |
| | 368 | 299 | 312 | 307 | 308 | 307 | 309 | 59 |
| | 485 | 315 | 328 | 323 | 331 | 325 | 323 | 162 |
| | 565 | 321 | 336 | 329 | 343 | 332 | 327 | 238 |
| Butanol | 295 | 291 | 293 | 292 | 292 | 292 | 293 | 2 |
| | 368 | 325 | 337 | 328 | 328 | 330 | 329 | 33 |
| | 485 | 346 | 363 | 351 | 358 | 351 | 355 | 130 |
| | 565 | 355 | 372 | 359 | 374 | 362 | 361 | 204 |
| 50% Ethanol + + 50% Butanol | 295 | 282 | 287 | 285 | 285 | 285 | 288 | 7 |
| | 368 | 304 | 318 | 312 | 314 | 313 | 318 | 50 |
| | 485 | 319 | 334 | 330 | 338 | 332 | 339 | 146 |
| | 565 | 327 | 342 | 337 | 351 | 340 | 347 | 218 |

of our approach that allowed such a restriction to be made.

In particular, at low ambient temperatures $T_{g\infty} < < T_b$, the droplet temperature differs little from $T_{g\infty}$: $T_{g\infty} - T_s \ll T_{g\infty}$. Then the quantity $c_{pg}(T_{g\infty} - T_s) \ll L_1 Z_1 + L_2 Z_2$ and $Y_{1s} + Y_{2s} \ll 1$. In this case, the expression for determining the evaporation temperature looks like

$$\frac{c_{pg}(T_{g\infty} - T_s)}{L_1 Z_1 + L_2 Z_2} = \frac{\mathrm{Sh}}{\mathrm{Nu}} \mathrm{Le}(Y_{1s} + Y_{2s}),$$

whence

$$T_{g\infty} = T_s + \frac{L_1 Z_1 + L_2 Z_2}{c_{pg}} \frac{\mathrm{Sh}}{\mathrm{Nu}} \mathrm{Le}(Y_{1s} + Y_{2s}). \quad (20)$$

However, already at ambient temperatures above 500 K, the application of this expression leads to considerable errors (see Table). It is so, because, as the temperature increases, the sum $Y_{1s} + Y_{2s} \to 1$ and the influence of the Stefan flow from the droplet surface, which is not taken into account in formula (20,), becomes substantial. The total evaporation rate increases, which should decrease the droplet temperature.

It is more classic to use the Newton–Richmann law without taking the Stefan flow into account. Then the equation for the evaporation temperature looks like

$$\frac{c_{pg}(T_{g\infty} - T_s)}{L_1 Z_1 + L_2 Z_2} = \frac{\mathrm{Sh}}{\mathrm{Nu}} \mathrm{Le} \ln\left[\frac{1}{1 - (Y_{1s} + Y_{2s})}\right],$$

whence

$$T_{g\infty} = T_s + \frac{L_1 Z_1 + L_2 Z_2}{c_{pg}} \times$$

$$\times \frac{\mathrm{Sh}}{\mathrm{Nu}} \mathrm{Le} \ln\left(\frac{1}{1 - (Y_{1s} + Y_{2s})}\right). \quad (21)$$

Formula (19) makes it possible to evaluate the evaporation temperature of a droplet of the binary solution as well. However, as is shown in Figs. 2 and 3, the droplet temperature does not have a clearly pronounced plateau. From the data exhibited in Fig. 3, it is possible to distinguish the temperature at which the rate of temperature change considerably decreases. This is the conditionally the first inflection point in the time dependences of the droplet temperature (solid diamonds in Fig. 3). One can see that the experimental values of this temperature for the 50% ethanol + 50% butanol mixture are substantially higher than the calculated results. Such a discrepancy is explained by a change in the droplet composition. Namely, the alcohol fraction decreases significantly, when this inflection point is reached. Curve *2*, which was calculated for the 25-% molar fraction of ethanol, gives a better agreement.

In work [33], by the example of water evaporation, it was shown that the temperature difference between the droplet and the environment depends linearly on the temperature of the latter. In Fig. 4, *b*, the results of the numerical solution of Eq. (19) are presented. One can see that the linear character of the dependence of the difference $T_{g\infty} - T_s$ on $T_{g\infty}$ is observed at the environment temperatures higher than the liquid boiling point, $T_g > T_b$ (Fig. 4, *b*).

In Table, the evaporation temperature values for the droplets of ethanol, butanol, and their 50/50 wt%

solution are quoted, which were obtained by numerically solving the system of equations (5) and (17), calculated according to formulas (19)–(21), and obtained experimentally. In general, a good agreement is observed for monofuel droplets. In the case of evaporation of the droplets of binary solutions, the temperatures at which their quasi-stationary evaporation with a low rate of temperature increase begins are 5–10 K higher than the calculated ones.

In the considered model, the influence of the heat supply through the thermocouple increases the stationary evaporation temperature of the droplet by 5%. As one can see, the experimental value lies between the two values obtained numerically.

## 7. Conclusions

The numerical simulation of the evaporation of a droplet of a bicomponent fuel in air heated above the boiling point of the most volatile component has made it possible to reveal some features in the evolution of the temperature and the squared diameter of the droplet. It is shown that the corresponding curves have two inflection points, which are associated with the competitive processes of the droplet composition change and the droplet temperature increase. As it takes place in the case where a droplet evaporates in air at room temperature, the evaporation of the droplet of a binary fuel can be divided into two stages according to the position of the second inflection point in the time dependence of the droplet temperature: 1) the simultaneous evaporation of both liquids with a dominating contribution of the more volatile substance and 2) the evaporation of the less volatile component.

A formula is proposed for the analytic determination of the temperatures of the droplets of one- and two-component liquid fuels in heated air with regard for the temperature dependence of the vaporization heat and the Lewis number.

The obtained results can be useful in further studies dealing with the evaporation and ignition of multicomponent fuels based on the diesel fuel, alcohols (including bioalcohols), and biolubricants. By varying the composition of the fuel mixture, it is possible to affect the main characteristics of the ignition and combustion processes of liquid multicomponent biofuels, and, as a result, minimize the fuel consumption and improve the environmental performance of combustion products in internal combustion engines without making any structural changes in them.

1. Chan Ho Jeong, Hyung Ju Lee, Chang Kyoung Choi, Seong Hyuk Lee. Review of the binary mixture droplet evaporation studies. *J. Mech. Sci. Technol.* **35**, 12 (2021).
2. D. Brutin, V. Starov. Recent advances in droplet wetting and evaporation. *Chem. Soc. Rev.* **47**, 558 (2018).
3. P. Gurrala, S. Balusamy, S. Banerjee, K.C. Sahu. A review on the evaporation dynamics of sessile drops of binary mixtures: challenges and opportunities. *Fluid Dynam. Mater. Process.* **17**, 253 (2021).
4. M. Sharma, S.S. Mondal, P.K. Roy, K. Khare. Evaporation dynamics of pure and binary mixture drops on dry and lubricant coated slippery surfaces. *J. Colloid Interf. Sci.* **569**, 244 (2020).
5. P. Chen, M. Toubal, J. Carlier, S. Harmand, B. Nongaillard, M. Bigerelle. Binary sessile drops evaporation: IR and acoustic methods for alcohol concentration tracking at the interface and the surface. *Langmuir* **32**, 9836 (2016).
6. T. Ozturk, H.Y. Erbil. Simple model for diffusion-limited droplet evaporation of binary liquids from physical properties of the components: ethanol-water example. *Langmuir* **36**, 1357 (2020).
7. K. Sefiane, S. David, M.E.R. Shanahan. Wetting and evaporation of binary mixture drops. *J. Phys. Chem. B* **112**, 11317 (2008).
8. P. Gurrala, P. Katre, S. Balusamy, S. Banerjee, K.C. Sahu. Evaporation of ethanol-water sessile droplet of different compositions at an elevated substrate temperature. *Int. J. Heat Mass Transf.* **145**, 118770 (2019).
9. A.A. Pahlavan, L. Yang, C.D. Bain, H.A. Stone. Evaporation of binary-mixture liquid droplets: the formation of picoliter pancakelike shapes. *Phys. Rev. Lett.* **127**, 024501 (2021).
10. E.L. Talbot, H.N. Yow, L. Yang, A. Berson, S.R. Biggs, C.D. Bain. Printing small dots from large drops. *ACS Appl. Mater. Inter.* **7**, 3782 (2015).
11. L. Urruty, M. Montury. Extraction in aqueous solutions by solid-phase microextraction. *J. Agric. Food Chem.* **44**, 3871 (1996).
12. L. Bahmani, M. Neysari, M. Maleki. The study of drying and pattern formation of whole human blood drops and the effect of thalassaemia and neonatal jaundice on the patterns. *Colloid. Surface. A* **513**, 66 (2017).
13. G. Strotos, I. Malgarinos, N. Nikolopoulos, M. Gavaises. Predicting the evaporation rate of stationary droplets with the VOF methodology for a wide range of ambient temperature conditions. *Int. J. Therm. Sci.* **109**, 253 (2016).
14. L.A. Bulavin, G.M. Verbinska, A.V. Brytan, Ya.O. Stepowyi. Model for evaporation of droplets of ideal alcohol solutions in diffusive and transient regimes. *Ukr. J. Phys.* **67**, 592 (2022).

15. O.V. Korobko, A.M. Brytan, G.M. Verbinska, D.A. Gav-ryushenko. Effect of ultraviolet radiation on evaporation of suspended alcohol droplets. *Ukr. J. Phys.* **60**, 318 (2019).

16. V. S. Savenko, G.M. Verbinska, L.A. Bulavin. Computer simulation of evaporation process of NaCl aqueous solution. *Ukr. J. Phys.* **61**, 812 (2019).

17. S. Sazhin. *Droplets and Sprays* (Springer Verlag, 2014).

18. A.K. Agarwal. Biofuels (alcohols and biodiesel) applications as fuels for internal combustion engines. *Prog. Energ. Combust.* **33**, 233 (2007).

19. Q.S. Khan, S.W. Baek. Effects of high ambient pressure and temperature on the autoignition of blended fuel droplets. In: *International Conference on Energy and Environment 2006* (ICEE, 2006), p. 56.

20. D. Segawa, T. Kadota, R. Kohama, H. Enomoto. Ignition of binary mixture droplets by a propagating laminar flame. *Proc. Combust. Inst.* **28**, 961 (2000).

21. R.S. Volkov, G.V. Kuznetsov, V.E. Nakoryakov, P.A. Strizhak. Experimental estimation of evaporation rates of water droplets in high-temperature gases. *J. Appl. Mech. Tech. Phys.* **58**, 889 (2017).

22. T. Kitano, J. Nishio, R. Kurose, S. Komori. Evaporation and combustion of multicomponent fuel droplets. *Fuel* **136**, 219 (2014).

23. T. Harada, H. Watanabe, Y. Suzuki, H. Kamata, Y. Matsushita, H. Aoki, T. Miura. A numerical investigation of evaporation characteristics of a fuel droplet suspended from a thermocouple. *Int. J. Heat Mass Transf.* **54**, 649 (2011).

24. O.V. Vysokomornaya, G.V. Kuznetsov, P.A. Strizhak. Evaporation of water droplets in a high-temperature gaseous medium. *J. Eng. Phys. Thermophys.* **89**, 141 (2016).

25. D. Fredrich, A. Giusti. Numerical investigation of multicomponent droplet evaporation and autoignition for aeroengine applications. *Combust Flame* **241**, 112023 (2022).

26. S.M. Frolov, F.S. Frolov, Ǎ20. Basara. Simple model of transient droplet vaporization. *J. Russ. Laser Res.* **27**, 562 (2006).

27. I. Veza, M.F.M. Said, Z.A. Latiff. Progress of acetone-butanol-ethanol (ABE) as biofuel in gasoline and diesel engine: A review. *Fuel Process. Technol.* **196**, 106179 (2019).

28. N. Yilmaz, E. Ileri, A. Atmanli. Performance of biodiesel/higher alcohols blends in a diesel engine. *Int. J. Energ. Res.* **40**, 1134 (2016).

29. O.S. Chernenko, V.V. Kalinchak, D.S. Darakov, O.K. Kopeck. The effect of suspension on the kinetics of evaporation of a droplet of liquid fuel. *Phys. Aerosol Syst.* **52**, 47 (2015).

30. K.M. Watson. Thermodynamics of the liquid state. *Ind. Eng. Chem.* **35**, 398 (1943).

31. A.N. Baratov, A.Ya. Korolchenko, G.N. Kravchuk. *Fire and Explosion Hazard of Substances and Materials, and Relevant Suppressants* (Khimiya, 1990) (in Russian).

32. D. R. Lide. *CRC Handbook of Chemistry and Physics.* 85th Edition. Vol. 85. (CRC Press, Jun 29, 2004).

33. A. Vinogradov, O. Yakhno. Effect of droplets convective heating and their evaporation on the shielding properties of fire-fighting water curtain. *Visn. NTUU KPI Ser. Mashynobud.* No. 2, 55 (2016) (in Russian).

*О.К. Копійка, В.В. Калінчак, О.С. Черненко*

ВИПАРОВУВАННЯ КРАПЕЛЬ
БІНАРНИХ СУМІШЕЙ НИЖЧИХ
ОДНОАТОМНИХ СПИРТІВ
У НАГРІТОМУ ПОВІТРІ

Представлені результати дослідження процесу випаровування одиночних крапель нижчих спиртів – етанолу, бутанолу та їх бінарних сумішей з початковим розміром крапель 1,5–2,5 мм у нагрітому повітрі при атмосферному тиску. Показано, що друга точка перегину на часовій залежності температури і квадрата діаметра дозволяє розділити час випаровування на дві стадії: 1) одночасне випаровування обох спиртів з переважним вмістом більш летючого спирту та 2) стадії випаровування важколетючого спирту. Термопара, що в умовах експерименту нагрівалася в печі, приводила до зменшення часу випаровування краплі і збільшення стаціонарної температури випаровування краплі. При температурах повітря, вищих за температуру кипіння рідинного палива різниця між температурами газового середовища і поверхні краплі, що випаровується, лінійно залежить від температури газового середовища. Запропоновано формулу для розрахунку в нагрітому повітрі температури випаровування краплі бінарного розчину, що дозволяє оцінити температуру, при якій починається квазістаціонарне випаровування краплі з малою швидкістю збільшення температури. При розрахунках використовувалася температурна залежність питомої теплоти пароутворення та відмінність числа Льюїса від одиниці. Наголошується на необхідності врахування течії Стефана в фізико-математичному моделюванні.

*К л ю ч о в і   с л о в а*: випаровування, спирти, розчин, крапля, термопара.